

Energy transfer properties and absorption spectra of the FMO complex: From exact PIMC calculations to TCL master equations

Piet Schijven,^{*} Lothar Mühlbacher,^{*} and Oliver Mülken^{*}

*Physikalisches Institut, Universität Freiburg, Hermann-Herder-Strasse 3, 79104 Freiburg,
Germany*

E-mail: petrus.schijven@physik.uni-freiburg.de; lothar.muehlbacher@physik.uni-freiburg.de;
muelken@physik.uni-freiburg.de

^{*}To whom correspondence should be addressed

Abstract

We investigate the excitonic energy transfer (EET) in the Fenna-Matthews-Olsen complex and obtain the linear absorption spectrum (at 300 K) by a phenomenological time-convolutionless (TCL) master equation which is validated by utilizing Path Integral Monte Carlo (PIMC) simulations. By applying Marcus' theory for choosing the proper Lindblad operators for the long-time incoherent hopping process and using local non-Markovian dephasing rates, our model shows very good agreement with the PIMC results for EET. It also correctly reproduces the linear absorption spectrum that is found in experiment, without using any fitting parameters.

Introduction

Since the seminal experiments on the Fenna-Matthews-Olsen (FMO) complex performed by the Fleming group in 2007¹ and subsequently confirmed by the Engel group in 2010,² many theoretical models have been proposed in order to properly describe the observed long-lasting oscillations in the 2D spectroscopic data. While many methods are based on quantum master equations of some sort or the other, like Lindblad or Redfield equations,^{3–6} only recently a more detailed description of dissipative effects has been attempted in the form of Path Integral Monte Carlo (PIMC) calculations based on results from atomistic modelling combining molecular-dynamics (MD) simulations with electronic structure calculations.⁷ In contrast to a phenomenological modelling of the “environment” (protein scaffold, water molecules, etc.), the latter approach utilizes BChl-resolved spectral densities which can be directly incorporated in the PIMC calculations to obtain an exact account of the full exciton dynamics.

Most quantum master equation approaches use special analytical forms of spectral densities, such as Ohmic or Lorentzian forms. Although this allows to obtain solutions for the equations, it remains to be a phenomenological ansatz. So far the results that have been obtained by hierarchical time-nonlocal master equations with a Lorentzian spectral density show reasonable agreement with the experimental results of both the absorption and 2D spectra at 77 K.^{8,9}

In contrast, numerically exact methods like PIMC simulations¹⁰ or the QUAPI method^{11–13}

have proven to be capable to produce the exact quantum dynamics of excitonic energy transfer over the experimentally relevant timescales. However, this comes at the price of rather large computational costs. Here, we combine the respective strenghts of numerically exact and approximate methods while overcoming their respective weaknesses: we use PIMC results for the exact quantum dynamics of the excitonic population dynamics over intermediate timescales (i.e. 600fs) which still allow for a fast production of the respective results, yet are sufficient to allow for a comparison to a time-convolutionless (TCL) master equation based on a Lindblad approach; we further corroborate our results by comparison with PIMC data for up to 1.5 ps. For a model dimer systems the authors have already successfully demonstrated such a concept.¹⁴ Here, our ansatz captures the long-time behavior by relating to Marcus' theory of electron transport^{15,16} because we assume that the long-time behaviour is governed by a classical hopping process between the individual sites,^{16,17} see below. For the short-time dephasing behavior we introduce non-Markovian dephasing rates.¹⁸ Since, in principle, we then obtain results for arbitrarily long times, we have an efficient yet very accurate way to calculate arbitrary transfer properties. Furthermore, we use the master equation to calculate the absorption spectrum of the FMO complex (at 300 K), an observable which can straightforwardly be obtained experimentally.¹⁹ This opens the possibility to estimate the validity of the underlying microscopic Hamiltonian as well as its respective parametrization based on recent results from mixed quantum-classical simulations²⁰ by getting into direct contact with experimental data.

Energy transfer on the FMO complex

Microscopic description The dynamics of single excitations on the FMO complex is often described by a tight-binding Hamiltonian with 7 localized sites, corresponding to the 7 bacteriochlorophylls (BChls) of the FMO monomer.^{21,22} The influence of the protein scaffold and solvent on the excitonic dynamics is treated, in the spirit of the Caldeira-Leggett model,²³ as a collection of harmonic modes that are linearly coupled to each BChl. Previous studies showed no significant

correlations between the bath induced energy fluctuations at different sites,^{24,25} so we assume that each BChl is coupled to its own individual environment. The full Hamiltonian of the system can now be written as:

$$H = H_S + H_B + H_{SB}, \quad (1)$$

with

$$H_S = \sum_n \varepsilon_n |n\rangle \langle n| + \sum_{m \neq n} J_{mn} |m\rangle \langle n|, \quad (2)$$

$$H_B = \sum_{n,\kappa} \left(\frac{P_{n\kappa}^2}{2m_{n\kappa}} + \frac{1}{2} m_{n\kappa} \omega_{n\kappa}^2 X_{n\kappa}^2 \right), \quad (3)$$

$$H_{SB} = \sum_n |n\rangle \langle n| \left(c_{n\kappa} X_{n\kappa} + \Lambda_n^{(\text{cl})} \right). \quad (4)$$

The state $|n\rangle$ corresponds to the single-excitation state of site n , the parameter ε_n denotes the energy gap between ground and excited state of site n , and J_{mn} describes the excitonic coupling between sites m and n . Furthermore, $X_{n\kappa}$, $P_{n\kappa}$, $m_{n\kappa}$ and $\omega_{n\kappa}$ denote the position, momentum, mass and frequency of the bath oscillators, respectively. In the interaction Hamiltonian H_{SB} , the constants $c_{n\kappa}$ (in units of eV/m) denote the coupling strength between site n and the bath modes. We have included the classical reorganization energies $\Lambda_n^{(\text{cl})}$ as a counter-term in H_{SB} to prevent further renormalization of the site energies by the environment.^{18,23,26} This quantity is defined as:

$$\Lambda_n^{(\text{cl})} = \frac{\hbar}{\pi} \int_0^\infty d\omega \frac{J_n(\omega)}{\omega}, \quad (5)$$

where $J_n(\omega)$ (in units of 1/s) is the spectral density of the bath that is coupled to site n . In terms of the system parameters, it is given by:

$$J_n(\omega) = \frac{\pi}{\hbar} \sum_{\kappa} \frac{c_{n\kappa}^2}{2m_{n\kappa}\omega_{n\kappa}} \delta(\omega - \omega_{n\kappa}). \quad (6)$$

The precise numerical values of the different parameters entering in the expressions above were obtained from combined quantum-classical simulations for the full FMO complex including the

solvent.^{20,27}

Effective master equation approach

We now use the microscopic description of the FMO complex to set up a phenomenological second order time-local quantum master equation. In doing so, we are able to reproduce the dynamics obtained from the PIMC simulations as well as extending it to, in principle, arbitrary long times. Additionally, our approach also allows to obtain results for the linear absorption spectrum which are in close accordance to experimental findings.

The spectral density of the FMO complex²⁰ leads to reorganisation energies $\Lambda_n^{(\text{cl})}$ of the order of 0.02 – 0.09 eV, which is comparable to the differences in the site energies ϵ_n , while the excitonic couplings J_{mn} are of the order of 1 meV. This implies that we can expect that the protein environment is relatively strongly coupled to the FMO complex and that it therefore leads to a strong damping for the population dynamics. This is also reflected by the results of the PIMC simulations.⁷

We now assume that in the long-time limit, after most of the coherences (i.e. off-diagonal elements of the reduced density matrix in the site-basis representation) in the system have decayed, EET can be described by a classical hopping process between the different sites (BChl's), that is induced by the protein environment. The transfer rates k_{mn} have to satisfy detailed balance, ensuring a correct equilibrium state, and are assumed to follow from Fermi's golden rule. Furthermore, the rates should also depend on the reorganisation energies $\Lambda_n^{(\text{cl})}$ and $\Lambda_m^{(\text{cl})}$ of the baths that are coupled to the sites n and m , reflecting the differences in the coupling strengths of the protein environment to each BChl. Unlike Förster theory, which assumes incoherent hopping between the energy eigenstates of H_s ,²⁸ Marcus's theory of electron transport satisfies all these properties,^{15,16} leading to transfer rates k_{mn} of the form:

$$k_{mn} = \sqrt{\frac{\pi\beta}{\hbar^2 \Lambda_{mn}^{(\text{cl})}}} |J_{mn}|^2 \exp \left[-\frac{\beta(\epsilon_n - \epsilon_m + \Lambda_{mn}^{(\text{cl})})^2}{4\Lambda_{mn}^{(\text{cl})}} \right], \quad (7)$$

with $\beta = 1/k_B T$ and $\Lambda_{mn}^{(\text{cl})} = \Lambda_m^{(\text{cl})} + \Lambda_n^{(\text{cl})}$.

Aside from incoherent transfer between the sites, the environment also induces a strong dephasing on each site. In the framework of the second order TCL master equation,¹⁸ these dephasing rates (in units of 1/fs) are given by:

$$\lambda_n(t) = 2\text{Re} \int_0^t ds \int_0^\infty d\omega J_n(\omega) [\coth(\beta\hbar\omega/2) \cos(\omega s) - i \sin(\omega s)]. \quad (8)$$

Here, we use the spectral densities $J_n(\omega)$ which have been obtained by MD simulations in Ref.²⁰ and numerically calculate the correlation function.

The TCL master equation that describes the excitation dynamics can now be written as:¹⁸

$$\frac{d\rho(t)}{dt} \equiv \mathcal{L}(t)\rho(t) = -\frac{i}{\hbar}[H_s, \rho(t)] + \mathcal{D}(t)\rho(t). \quad (9)$$

Our numerical results (not displayed) show that the Lamb shift term that usually appears in this equation, only leads to a negligible difference in both the population dynamics and the linear absorption spectrum (the position of the peak is shifted by approximately -1 meV). The dissipator $\mathcal{D}(t)$ is assumed to take the following Lindblad form, according to the considerations above:¹⁸

$$\mathcal{D}(t)\rho(t) = \sum_{mn} \gamma_{mn}(t) \left(L_{mn}\rho L_{mn}^\dagger - \frac{1}{2} \{ L_{mn}^\dagger L_{mn}, \rho \} \right). \quad (10)$$

The Lindblad operators are defined by $L_{mn} = |m\rangle\langle n|$ and the rates by $\gamma_{mm}(t) = \lambda_m(t)$ and $\gamma_{mn}(t) = k_{mn}$ for $m \neq n$. The operators L_{mm} model the dephasing process, while the operators L_{mn} model the incoherent transfer between sites m and n . This choice of Lindblad operators will lead - in the long-time limit - to incoherent hopping transfer between the sites, which is different from, e.g., Redfield theory, which requires incoherent transfer between the eigenstates $|\psi\rangle$ of H_s , leading to Lindblad operators of the form $L \sim |\psi_n\rangle\langle\psi_m|$.^{16,18}

However, we note that the equilibrium state of our master equation (ρ_{eq}) is slightly different from the one that follows from Marcus theory $\rho_{eq,db}$, which is given by detailed balance,

$\lim_{t \rightarrow \infty} \rho_{nn}(t) = (1/Z) \exp(-\beta \epsilon_n)$ and $\lim_{t \rightarrow \infty} \rho_{mn}(t) = 0$ for $m \neq n$, where $\rho_{mn}(t) = \langle m | \rho(t) | n \rangle$. This can be shown by noting that $\mathcal{D}(t) \rho_{eq,db} = 0$ but $[H_S, \rho_{eq,db}] \neq 0$. This implies that $\rho_{eq,db}$ is not a stationary state of our master equation. For the present calculation, the deviations are only of the order of 1%, so we still expect our approach to give good results.

Path Integral Monte Carlo simulations

PIMC simulations allow to extract the exact quantum dynamics in the presence of a dissipative environment, both for charge transport^{10,29,30} as well as energy transfer.⁷ In short, the time evolution of the reduced density operator of a dissipative quantum systems is calculated by employing the path integral representation for the propagator according to the Feynman-Vernon theory³¹ for factorizing or its extension to correlated initial preparations.³² These path integrals are then evaluated by a stochastic sampling process based on Markov walks through the configuration space of all conceivable quantum paths which self-consistently emphasize the physically most relevant ones. While there is no limitation with respect to the choice of system parameters for which PIMC simulation are capable of producing numerically exact results, this approach is subject to the notorious ‘dynamical sign problem’,³³ which reflects quantum-mechanical interferences between different system paths and results in an increase of the computational effort necessary to obtain statistically converged results which scales exponentially with the timescale over which the dynamics of the system is investigated. However, the presence of a dissipative environment substantially weakens these interference effects and therefore the sign problem. Furthermore, it allows for various efficient optimization schemes which lead to a further soothing of this computational bottleneck, thus significantly enlarging the accessible timescales.^{10,34,35}

For the present case, we utilize the PIMC data presented in Ref.⁷ to demonstrate the reliability of the master equation results and extend some of the former to longer timescales. To that extend, a factorizing initial preparation has been employed, where, resembling the situation prior to the creation of an exciton, the bath modes initially are in thermal equilibrium with respect to themselves, while the exciton has been modeled to be either initially localized on one of the seven BChl sites

or in one of the seven excitonic eigenstates.

Population dynamics

In Fig. 1 we show the population dynamics that is obtained by solving the TCL master equation, Eq. (9), for initial conditions corresponding to a localization on the sites $|n\rangle$, e.g. $\rho(0) = |n\rangle\langle n|$, in comparison to the corresponding numerically exact PIMC results. The dotted curves represents the latter and the solid lines represent the results from our master equation approach. Fig. 2 shows an extension of the results up to 1200 and 1500 fs for initial preparations in sites 1 and 6, respectively.

In general we observe good quantitative agreement of our approach with the PIMC results for all localized initial preparations and over all observed timescales. The largest deviations are observed for an initial condition localized on site 4 for which the bath has the lowest reorganization energy (0.025 eV). Since our assumption of a classical hopping process at long-times is based on having a strong coupling to the environment, we would expect that our approach becomes worse with decreasing reorganisation energy. Also, from Fig. 2 one observes a good agreement in the approach to equilibrium, although the decay is slightly slower than predicted by the PIMC results.

Figure 3 corroborates our results. Here, the excitonic excitation is initially in one of the seven eigenstates $|\psi_n\rangle$ of H_S . Again we find very good agreement with the PIMC results, where once more the strongest deviations occur for the initial preparation exhibiting the largest population on site 4. We note that there is no fitting parameter involved. Introducing a parameter which interpolates between purely coherent and purely incoherent transfer, as in,^{36–38} could lead to a further improvement of the agreement. Nevertheless, already this rather simple phenomenological model captures most of the details which are present in the PIMC calculations. Additionally, it allows for a computationally cheap calculation of the linear absorption spectrum.

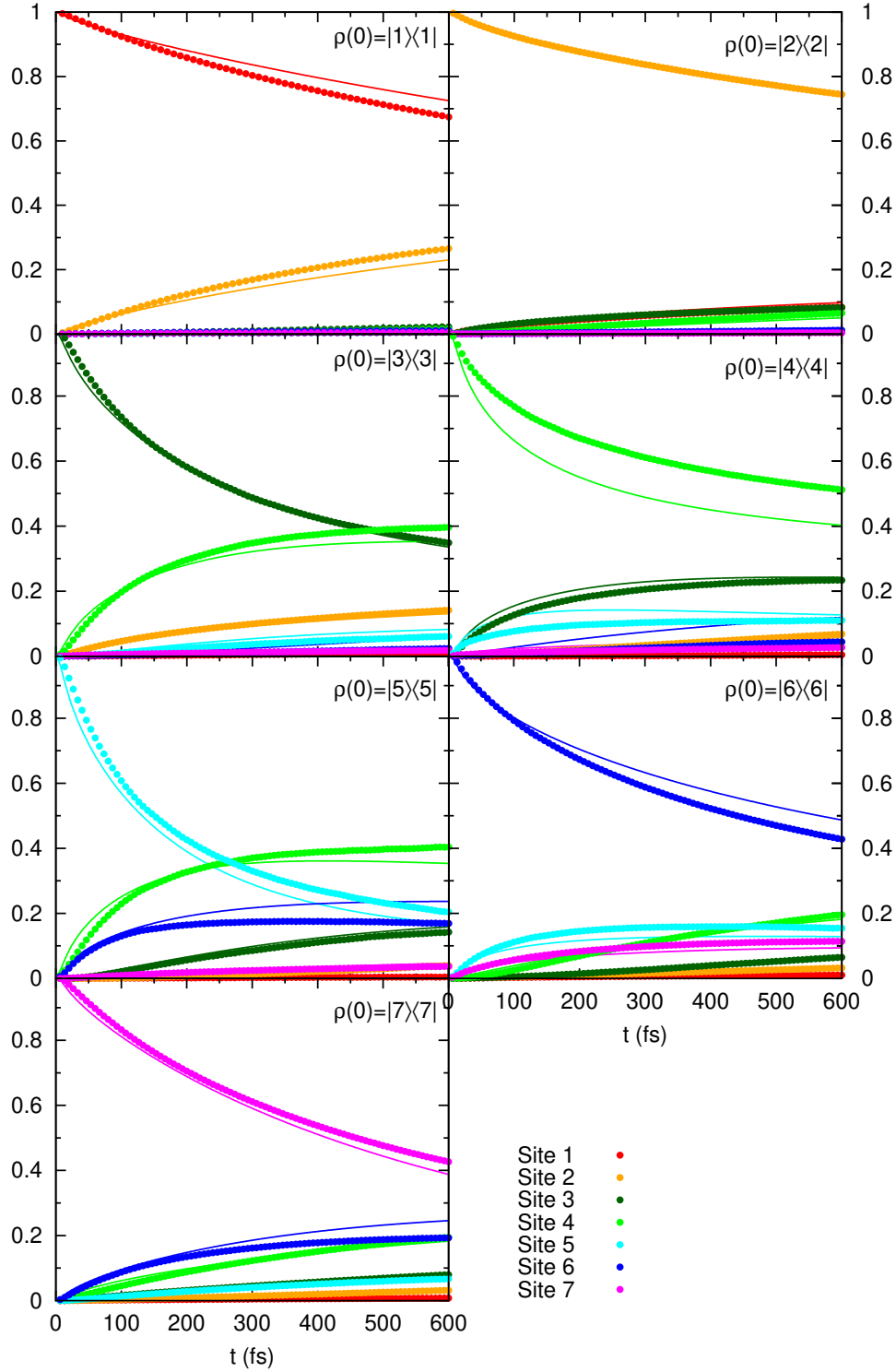


Figure 1: Comparison of population dynamics of the 7 different sites of the FMO complex obtained from the numerically exact PIMC results (circles) with the results from the TCL master equation approach (solid lines) for different localized initial conditions on the sites $|n\rangle$, $n = 1, \dots, 7$. Note that the statistical error of the PIMC calculations is typically smaller than the symbol size. Therefore we do not show the error bars.

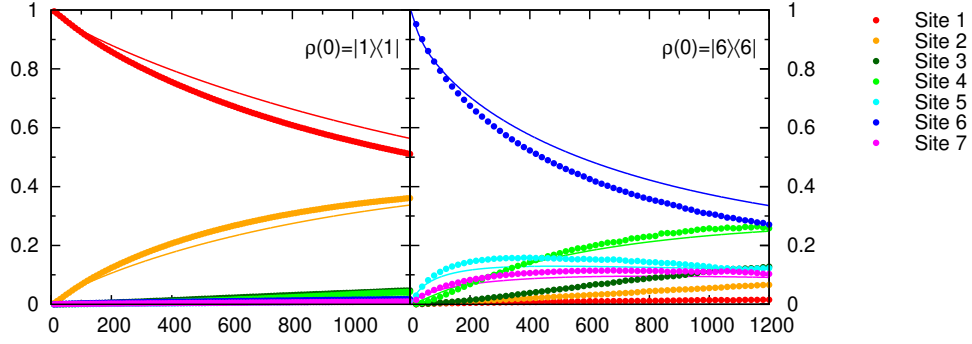


Figure 2: Same as Fig. 1 for localized initial preparations in sites 1 and 6, but now extended beyond 1ps

Table 1: The numerical values for the x-, y-, and z- component as well as the absolute value squared of the transition dipole moments $\vec{\mu}_m = (\mu_{m,x}, \mu_{m,y}, \mu_{m,z})$ in units of Debye $[D]$. The z axis is chosen along the C_3 -symmetry axis of the FMO complex, and the y axis is chosen to be parallel to the $N_B - N_D$ axis of BChl 1.

m	1	2	3	4	5	6	7
$\mu_{m,x}$	0.0	-6.10	-5.27	0.0	-6.39	5.16	0.0
$\mu_{m,y}$	1.86	1.08	-3.04	2.49	0.0	2.98	-1.14
$\mu_{m,z}$	6.07	1.66	-2.10	5.85	-0.45	2.29	5.85
$ \vec{\mu}_m ^2$	40.32	41.09	41.47	40.45	41.09	40.70	35.52

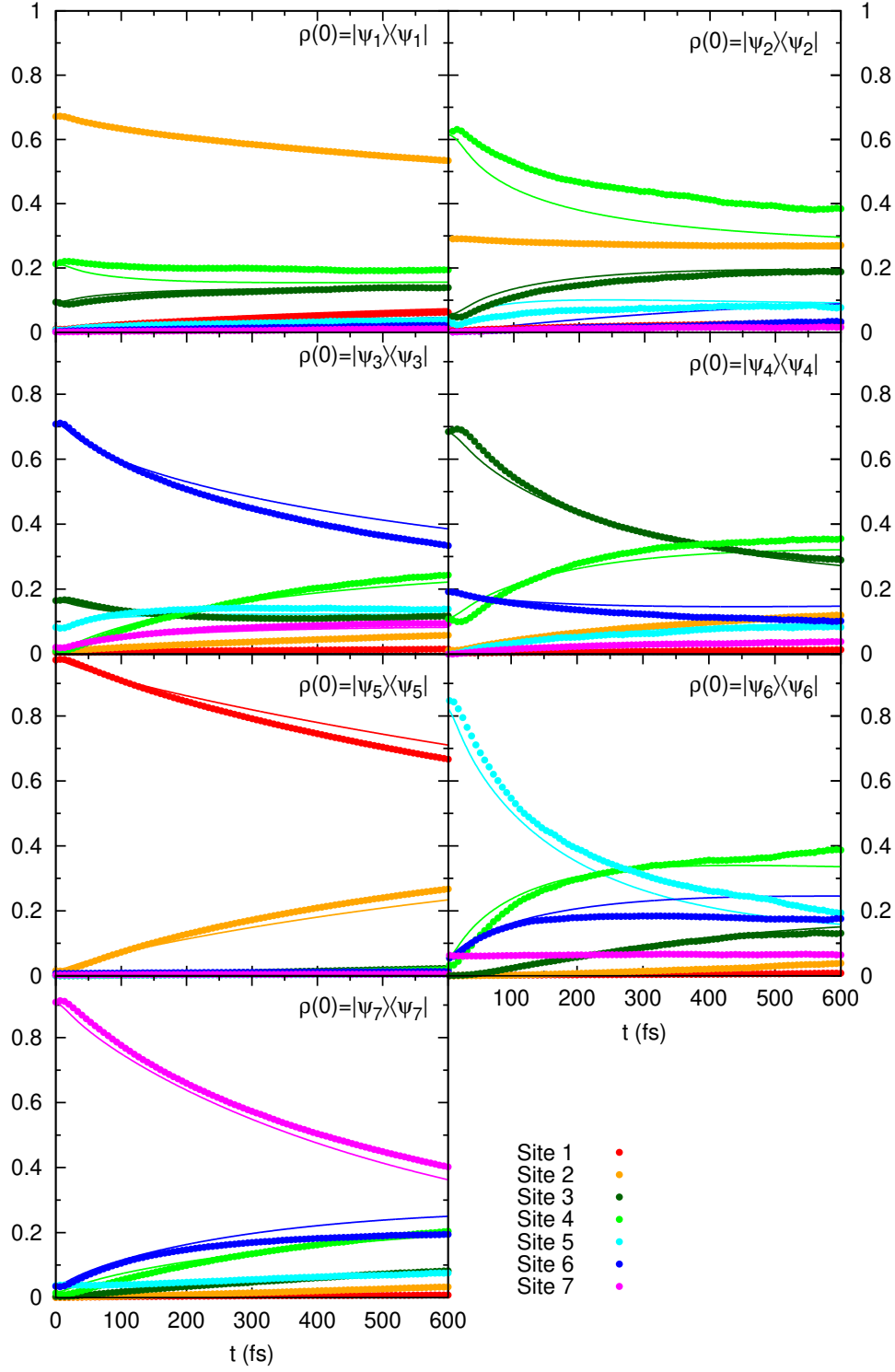


Figure 3: Same as Fig. 1 but taking the eigenstates $|\Psi_n\rangle$ of H_S as initial conditions.

Linear absorption spectrum

Due to the strong dephasing that is induced by the protein environment, the coherences (i.e., the off-diagonal elements of the reduced density matrix in the site basis) die out rather fast. Hence, the dynamics of the populations is mostly insensitive to the exact behaviour of the coherences. However, other observables, such as the linear absorption spectrum, are very sensitive to the short-time behavior, where the coherences are still present. Being able to access the full dynamics of the reduced density matrix for, in principle, arbitrary timescale, now allows us to access in particular the linear absorption spectrum for the FMO complex. We calculate the linear absorption spectrum and compare it to the absorption spectrum which was measured in experiment¹⁹ and to the one which has been computed with mixed quantum-classical simulations by Olbrich *et al.*²⁰

The linear absorption spectrum is given by the Fourier transform of the two-time correlation function of the transition dipole moment (TDM) operator $\vec{\mu}$:¹⁶

$$A(\omega) = \text{Re} \int_0^\infty dt e^{i\omega t} \langle \vec{\mu}(t) \cdot \vec{\mu}(0) \rangle, \quad (11)$$

where $\vec{\mu}(t) = e^{iHt/\hbar} \vec{\mu} e^{-iHt/\hbar}$ is the TDM operator in the Heisenberg picture and $\vec{\mu} = \sum_m \vec{\mu}_m (|m\rangle\langle 0| + |0\rangle\langle m|)$, with $\vec{\mu}_m$ the TDM vector of site m . The two-time correlation function is evaluated in the excitonic ground state $W^0 = |0\rangle\langle 0| \otimes \rho_B$, i.e., with no excitations present.

To compute this correlation function with our approach, we use the following expression:¹⁸

$$\langle \vec{\mu}(t) \cdot \vec{\mu}(0) \rangle = \text{tr}_S \left\{ \vec{\mu}(t) \cdot \vec{V}(t) \right\}, \quad (12)$$

where the vector-operator $\vec{V}(t)$ satisfies the TCL master equation

$$\frac{d\vec{V}(t)}{dt} = \mathcal{L}(t)\vec{V}(t), \quad (13)$$

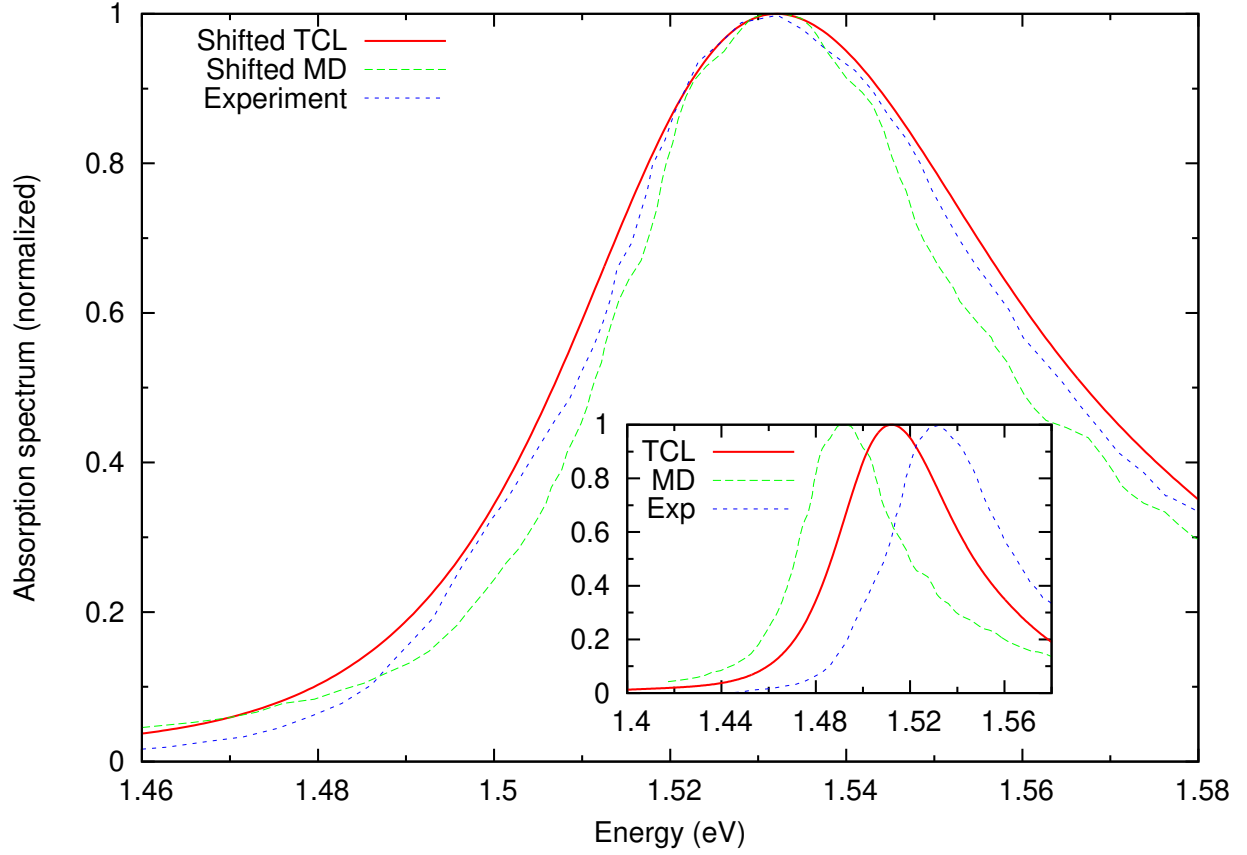


Figure 4: Comparison of the linear absorption spectra, computed with the TCL master equation (solid red), mixed quantum-classical calculations²⁰ (dashed green) and obtained by experiment¹⁹ (dotted blue). All three spectra are overlaid such that the position of the peaks are shifted to that of the experimental result. The inset shows the spectra at their original positions.

with the initial condition

$$\vec{V}(0) = \vec{\mu} \text{tr}_B \{W^0\} = \vec{\mu} |0\rangle\langle 0| = \sum_m \vec{\mu}_m |m\rangle\langle 0|, \quad (14)$$

where tr_S and tr_B denote the trace over the excitonic and environmental degrees of freedom, respectively. Due to the time dependence of the dephasing rates that enter into the generator $\mathcal{L}(t)$, we cannot obtain an analytical solution for the linear absorption spectrum. Therefore, we solve Eq. (13) numerically and obtain the absorption spectrum with Eq. (12).

The numerical values of the TDM vectors $\vec{\mu}_m$ are obtained by combining the data from Refs.²⁰ and ³⁹ together with their relative orientations with respect to the C_3 symmetry axis, taken from Ref.⁴⁰ In table 1 we provide the computed values of the $\vec{\mu}_m$'s.

In Fig. (4) we show the numerical results for the linear absorption spectrum and compare it to the experimental results by Freiberg *et. al.*¹⁹ and computational results obtained by Olbrich *et. al.*²⁰ utilizing the same parametrization of the Hamiltonian, Eq. (1), but based on ensemble-averaged wavepacket dynamics.⁴¹ We observe that both the spectra from the latter and from our theoretical approach are shifted by -0.04 eV and -0.02 eV, respectively, compared to the experimental spectrum. When overlaying those spectra such that the position of the peaks match, we observe almost perfect agreement for the overall actual lineshape, even though our method lacks the detailed features of the experiment. We note that our approach yields a shift from the experimental findings which is only half as large as the one presented in Ref.²⁰ This indicates that despite the strong dissipation, quantum effects still play an important role for the excitonic dynamics which are not captured by the ensemble-averaged wavepacket dynamics.

Summary

We have presented an approach to calculate the EET as well as the absorption spectrum of the FMO complex. Our approach is based on a phenomenological TCL master equation: The dissipator in the master equation is determined by incoherent hopping rates obtained from Marcus'

theory as well as by non-Markovian (pure) dephasing rates obtained from the bath autocorrelation function. Here, we have used spectral densities calculated from atomistic simulations of Ref.²⁷ We have demonstrated the quantitative reliability of our TCL master equation by a comparison with population dynamics obtained from numerically exact PIMC simulations exhibiting an excellent accuracy for timescales up to the picosecond range, both, for the exciton initially found localized on any BChl as well as in an excitonic eigenstate. Furthermore, we also found very good agreement with the experimentally measured absorption spectrum. Here, the overall lineshape of the absorption spectrum is reproduced very nicely, although the position of the peak is shifted by 0.02 eV as compared to the experimental result, yet considerably less than for calculations based on wavepacket dynamics. Since we have correctly reproduced both the population dynamics and the dynamics of the coherences, as reflected in the absorption spectrum, we also expect to be able to reproduce the results for 2D electronic spectroscopy that were found in experiments at ambient conditions, which is subject of current research.

Acknowledgement

We gratefully acknowledge support from the Deutsche Forschungsgemeinschaft (DFG grant MU2925/1-1 MU 2926/1-1). Furthermore, we thank A. Anishchenko, A. Blumen, and L. Lenz for useful discussions.

References

- (1) Engel, G.; Calhoun, T.; Read, E.; Ahn, T.; Mančal, T.; Cheng, Y.-C.; Blankenship, R.; Fleming, G. *Nat. Phys.* **2007**, *446*, 782–786.
- (2) Panitchayangkoon, G.; Hayes, D.; Fransted, K.; Caram, J.; Harel, E.; Wen, J.; Blankenship, R.; Engel, G. *P. Natl. Acad. Sci. USA* **2010**, *107*, 12766–12770.
- (3) Wu, J.; Liu, F.; Shen, Y.; Cao, J.; Silbey, R. *New. J. Phys* **2010**, *12*, 105012.
- (4) Palmieri, B.; Abramavicius, D.; Mukamel, S. *J. Chem. Phys.* **2009**, *130*, 204512.

- (5) Mohseni, M.; Rebentrost, P.; Lloyd, S.; Aspuru-Guzik, A. *J. Chem. Phys.* **2008**, *129*, 174106.
- (6) Rebentrost, P.; Mohseni, M.; Kassal, I.; Lloyd, S.; Aspuru-Guzik, A. *New. J. Phys.* **2009**, *11*, 033003.
- (7) Mühlbacher, L.; Kleinekathöfer, U. *J. Phys. Chem. B* **2012**, *116*, 3900–3906.
- (8) Chen, L.; Zheng, R.; Jing, Y.; Shi, Q. *J. Chem. Phys.* **2011**, *134*, 194508.
- (9) Hein, B.; Kreisbeck, C.; Kramer, T.; Rodríguez, M. *New. J. Phys.* **2012**, *14*, 023018.
- (10) Mühlbacher, L.; Ankerhold, J.; Escher, C. *J. Chem. Phys.* **2004**, *121*, 12696–12707.
- (11) Makri, N.; Makarov, D. *J. Chem. Phys.* **1995**, *102*, 4600–4610.
- (12) Makri, N.; Makarov, D. *J. Chem. Phys.* **1995**, *102*, 4611–4618.
- (13) Thorwart, M. *Chem. Phys.* **2004**, *296*, 333–344.
- (14) Mülken, O.; Mühlbacher, L.; Schmid, T.; Blumen, A. *Phys. Rev. E* **2010**, *81*, 041114.
- (15) Marcus, R. *J. Chem. Phys.* **1956**, *24*, 966–978.
- (16) Nitzan, A. *Chemical Dynamics in Condensed Phases: relaxation, transfer and reactions in condensed molecular systems*; Oxford graduate texts; Oxford University Press, 2006.
- (17) Ishizaki, A.; Fleming, G. R. *J. Phys. Chem. B* **2011**, *115*, 3227–6233.
- (18) Breuer, H.; Petruccione, F. *The theory of open quantum systems*; Oxford University Press, 2010.
- (19) Freiberg, A.; Lin, S.; Timpmann, K.; Blankenship, R. E. *J. Phys. Chem. B* **1997**, *101*, 7211–7220.
- (20) Olbrich, C.; Jansen, T. L. C.; Liebers, J.; Aghtar, M.; Strümpfer, J.; Schulten, K.; Knoester, J.; Kleinekathöfer, U. *J. Phys. Chem. B* **2011**, *115*, 8609–8621.

- (21) Fenna, R. E.; Matthews, B. W. *Nature* **1975**, 258, 573–577.
- (22) Brixner, T.; Stenger, J.; Vaswani, H.; Cho, M.; Blankenship, R.; Fleming, G. *Nature* **2005**, 434, 625–628.
- (23) Caldeira, A.; Leggett, A. *Ann. Phys.* **1983**, 149, 374–456.
- (24) Olbrich, C.; Strümpfer, J.; Schulten, K.; Kleinekathöfer, U. *J. Phys. Chem. B* **2011**, 115, 758–764.
- (25) Shim, S.; Rebentrost, P.; Valleau, S.; Aspuru-Guzik, A. *Biophysical Journal* **2012**, 102, 649–660.
- (26) Caldeira, A.; Leggett, A. *Ann. Phys.* **1984**, 153, 445.
- (27) Olbrich, C.; Strümpfer, J.; Schulten, K.; Kleinekathöfer, U. *J. Phys. Chem. Lett.* **2011**, 2, 1771–1776.
- (28) Förster, T. *Discuss. Faraday Soc.* **1959**, 27, 7–17.
- (29) Egger, R.; Mak, C.; Weiss, U. *Phys. Rev. E* **1994**, 50, 655.
- (30) Mühlbacher, L.; Ankerhold, J. *J. Chem. Phys.* **2005**, 122, 184715.
- (31) Feynman, R.; Vernon, F., Jr. *Ann. Phys.* **1963**, 24, 118–173.
- (32) Grabert, H.; Schramm, P.; Ingold, G.-L. *Phys. Rep.* **1988**, 168, 115–207.
- (33) Suzuki, M. *Quantum Monte Carlo methods in Condensed Matter Physics*; World Scientific: Singapore, New Jersey, London, Hong Kong, 1993.
- (34) Egger, R.; Mühlbacher, L.; Mak, C. *Phys. Rev. E* **2000**, 61, 5961–5966.
- (35) Stockburger, J.; Grabert, H. *Phys. Rev. Lett.* **2002**, 88, 170407.
- (36) Whitfield, J.; Rodriguez-Rosario, C. A.; Aspuru-Guzik, A. *Phys. Rev. A* **2010**, 81, 022323.

- (37) Schijven, P.; Kohlberger, J.; Blumen, A.; Mülken, O. *J. Phys. A: Math. Theor.* **2012**, *45*, 215003.
- (38) Schijven, P.; Mülken, O. *Phys. Rev. E* **2012**, *85*, 062102.
- (39) Li, Y.-F.; Zhou, W.; Blankenship, R. E.; Allen, J. P. *J. Mol. Biol.* **1997**, *271*, 456–471.
- (40) Milder, M. T. W.; Brüggemann, B.; van Grondelle, R.; Herek, J. L. *Photosynth. Res* **2010**, *104*, 257–274.
- (41) Parandekar, P. V.; Tully, J. C. *J. Chem. Theory Comput.* **2006**, *2*, 229–235.